energy for sulfur in zirconium sulfate ($Zr(SO_4)_2$), as obtained by Arata (51). Figure 61 show the spectrum of the zirconium $3d_{3/2}$ and $3d_{5/2}$ core levels. The separation by approximately 2 eV also follows the results Arata presented. These results confirm that the utilized preparation procedure indeed gave sulfated zirconia. The peaks in the spectra presented are broad due to charging of the sample. This phenomenon will always occur when XPS is performed on non-conducting materials. Charge compensation using a flood gun was used to minimize the charging effect.

E. Probing the Acidity of Sulfate-Modified Zirconia by XPS

The objective of these experiments was to investigate the acidic properties of sulfate-modified zirconia. An understanding of the acid function induced by the sulfate dopant might provide for further improvement of this very active catalyst for the high temperature (175°C) dehydration of isobutanol to isobutene and the low temperature (125°C) coupling of methanol and isobutanol to ethers. By adsorbing nitrogen-containing bases such as pyridine, on the catalyst surface, the presence and type of acidic species can be monitored by XPS N 1s core level shifts. The observed shifts of the N 1s binding energy line can be related to the strength with which the nitrogen-containing base is adsorpbed onto the surface. By this means, Lewis and Brönsted acid sites on the surface of this catalyst were distinguished and quantified. Water is a reaction product formed over the catalyst during isobutanol dehydration, as well as during ether synthesis, and probe the correlation of partial pressure of water over the catalyst to the ratio of Lewis to Brönsted sites, a water adsorption experiment was also carried out prior to adsorption of the pyridine adsorbate.

A new glass vacuum system was designed and constructed in our laboratory for the pretreatment of the sulfate-modified zirconia samples. The system was able to attain a

Figure 61. XPS of the zirconium 3d region of the ZrO_2/SO_4^{2-} catalyst.

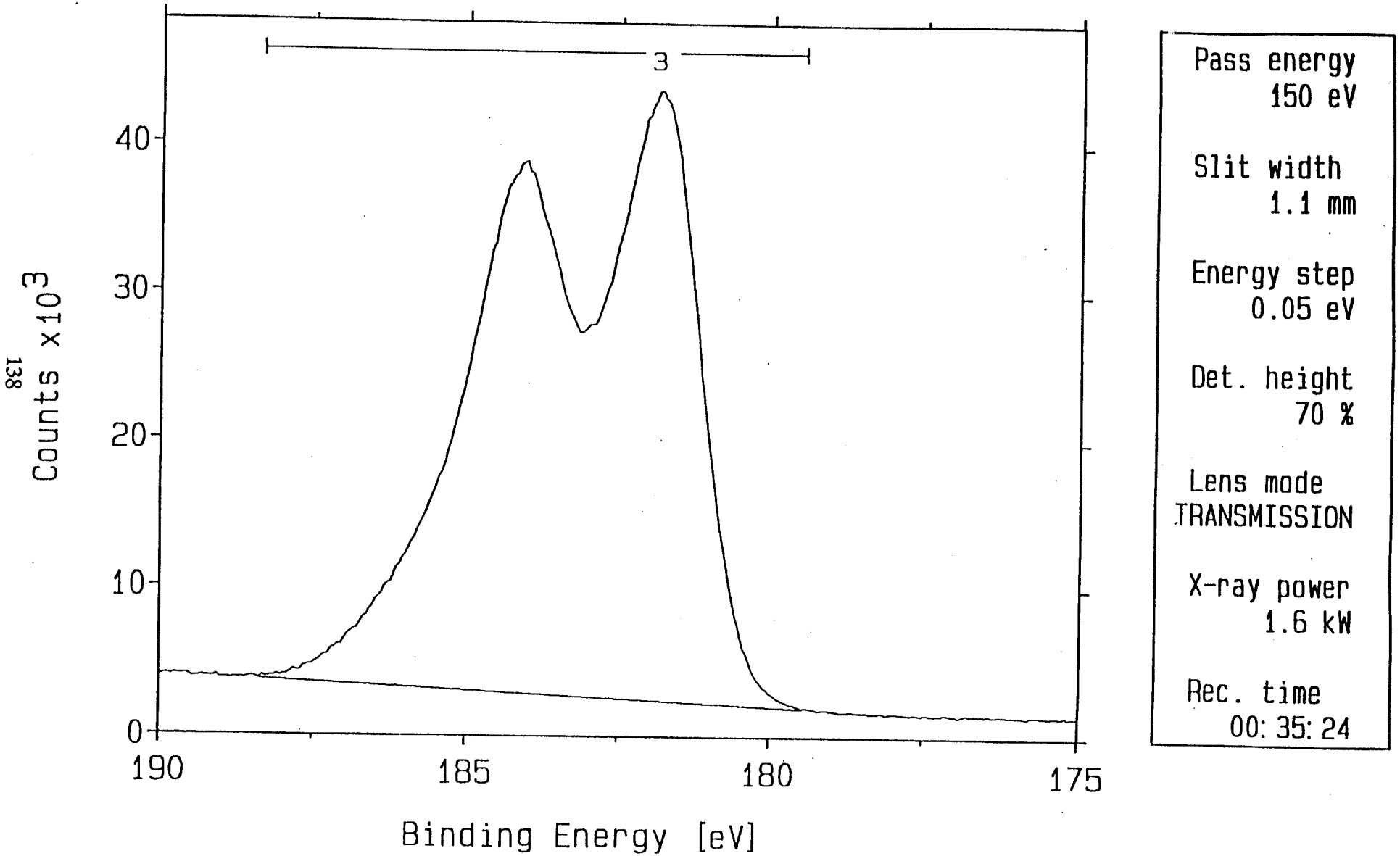

vacuum of 10^{-5}-10^{-6} torr. A schematic of the vacuum system is shown in Figure 62. External ovens were used to heat the sample as well as the adsorbates so that a constant designated vapor pressure of the individual adsorbates could be maintained. A new high precision digital pressure manometer was purchased to monitor the pressure of gas in the sample pretreatment, as well as to measure the uptake of pyridine during the experiments. The model 572 Barocel pressure sensor with a model 1174 electronic manometer from Edwards High Vacuum Int. can measure pressures from 0.001 torr to 1000 torr with 0.001 torr resolution.

The procedure used for the pretreatment of the catalyst prior to XPS analysis was as follows:

1. The sulfate-modified zirconia was freshly calcined at 620°C for 3 hr.
2. The sample was introduced into one of the glass tubes on the vacuum system under ambient conditions.
3. The sample was evacuated at 415°C for 1 hr.
4. The catalyst was then exposed to 15 torr of pyridine for 0.5 hr at 25°C.
5. Finally, the sulfate-modified zirconia was evacuated at 150°C for 1 hr to desorb excess physisorbed pyridine not chemisorbed to Brönsted or Lewis acid sites.

For the water-adsorption experiment, the following two steps were carried out after Step 3, but before Step 4, given above:

3a. Water vapor at 75 torr was allowed to adsorb onto and equilibrate with the catalyst at 175°C for an exposure time of 0.5 hr.

3b. The sample was then evacuated at 175°C for 1 hr.

Sample tubes with the teflon stopcocks closed and still in place were removed from the vacuum manifold and put into a glovebag purged with dry nitrogen gas. The sample tubes were opened in the glovebag, and the catalyst sample was mounted onto a sample

Figure 62. Schematic of the new high vacuum system for pretreatment of samples for XPS analysis.

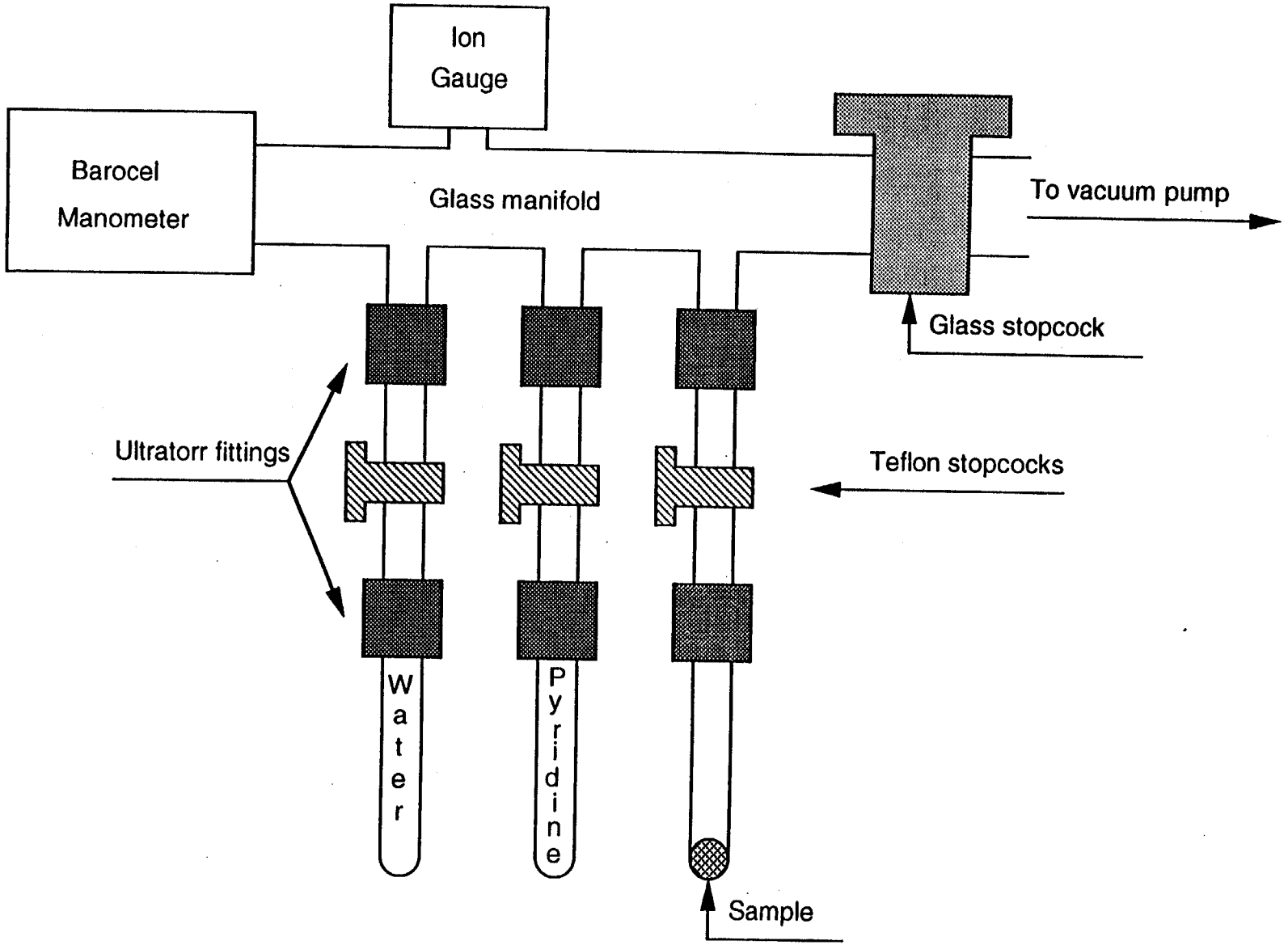

holder and introduced into the SCIENTA-300 ESCA instrument without exposure to air or moisture.

The nitrogen 1s binding energy is 398-400 eV for free pyridine compounds and pyridine coordinated to Lewis acid sites (54). The binding energy of N 1s increases to 400-402 eV for pyridinium compounds, such as pyridine protonated by a Brönsted acid (54).

The first sulfate-modified zirconia sample was pretreated according to Steps 1-5 given above. This sample is dry since no water was introduced. Figure 63 shows the N 1s XPS spectrum of pyridine adsorbed onto this dry SO_4^{2-}/ZrO_2 sample. There are two main peaks observed at 398.8 eV and 401.4 eV, and these correspond to pyridine coordinated to a Lewis acid site and to a Brönsted acid site, respectively. The line positions were referenced to Zr $3d_{5/2}$ = 182.3 eV, and a flood gun was used to reduce sample charging, which was minimized by manipulating the flood gun until the Zr 3d lines were as narrow as possible. The peak at 404.6 eV could be due to very strong Brönsted acid sites, but this has to be confirmed by further experiments. Pyridine as an aromatic compound could exibit final state effects, however when data of pyridine were taken on Nafion-H (see later Figure 66), the peak at very high binding energy was absent thus indicating that final state effects are only minor if present at all. If only the two peaks at lower binding energy are considered, the peak at 401.4 eV is 65% of the total peak area, whereas the peak at 398.8 eV makes up the remaining 35%. This means that for a dry sample, calcined to 620°C, the Brönsted acid sites are still the major contributor to the acidity of the sample. It should be noted that the pyridine used in this experiment was not exposed to moisture since it was packed and stored under nitrogen.

Following this experiment, a new SO_4^{2-}/ZeO_2 sample was pretreated and exposed to water vapor, as indicated by Steps 3a and 3b. Figure 64 shows the resultant N 1s XPS

Figure 63. XPS of the N 1s region of the dry ZrO_2/SO_4^{2-} catalyst with adsorbed pyridine.

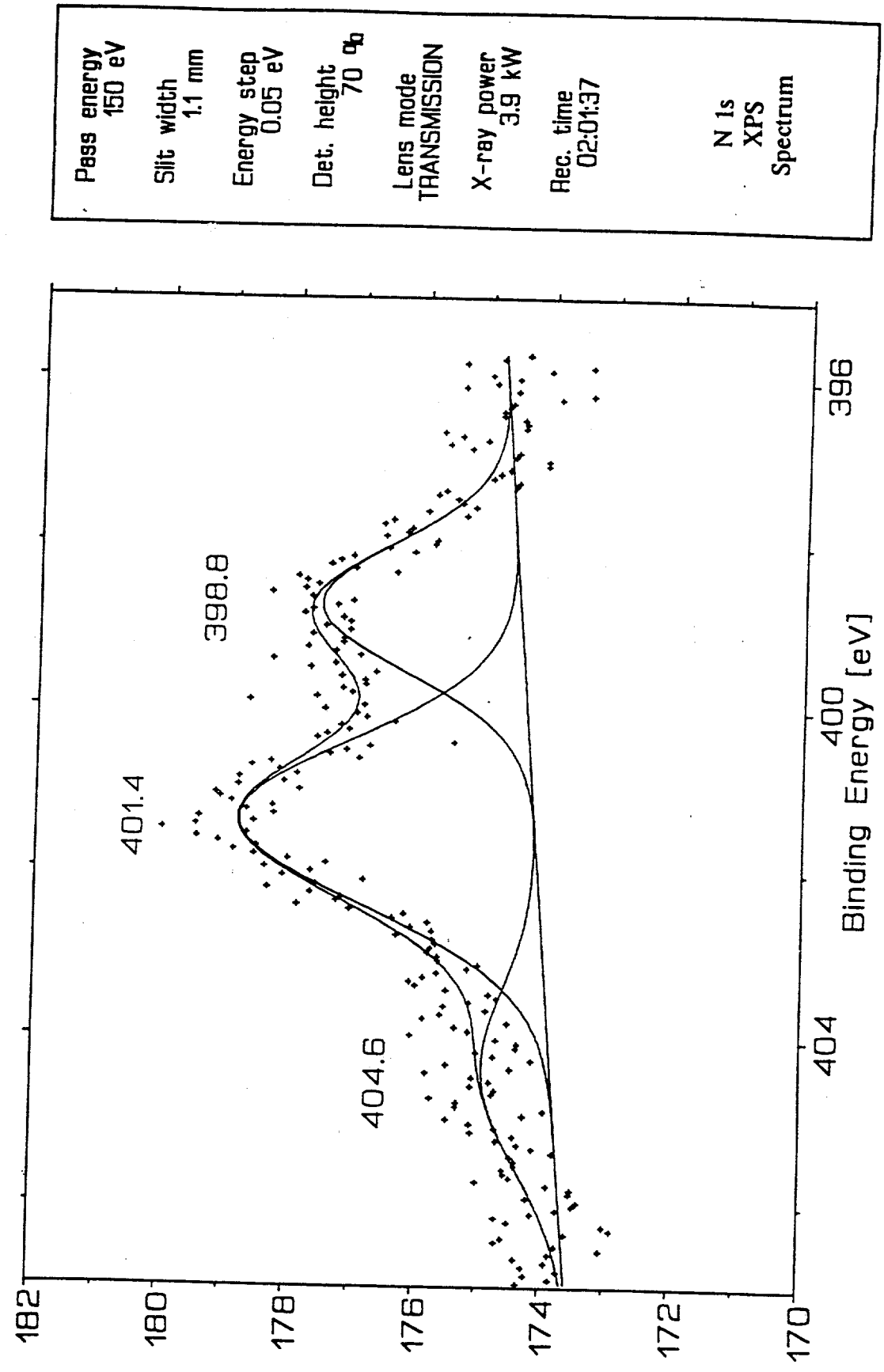

Figure 64. XPS of the N 1s region of the wet ZrO_2/SO_4^{2-} catalyst with adsorbed pyridine.

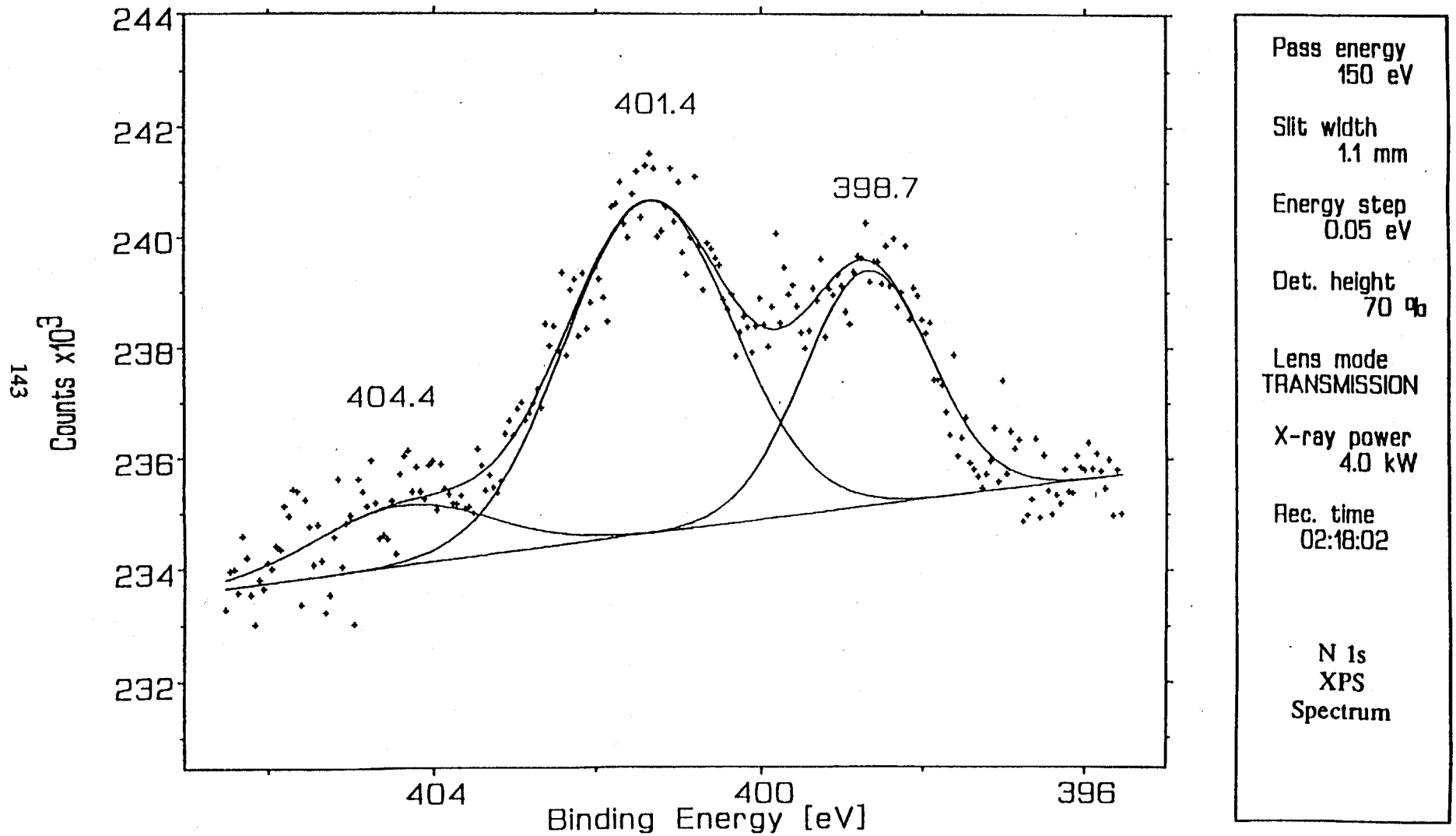

spectrum of this SO_4^{2-}/ZrO_2 sample. This sample is termed to be "wet" due to water admission prior to the pyridine adsorption. Again, the two main spectral peaks were observed at 398.7 eV and 401.4 eV, respectively. The same area percentages are seen for this wet sample as for the dry sample. The 401.4 eV peak corresponds to 64% of the total area, and the 398.7 eV peak is the remaining 36% provided that the peak at 404.4 eV is excluded as above.

These results indicate that even after calcination at 620°C for 3 hr, there is a significant quantity of Brönsted acid sites present on the catalyst surface. With the conditions used in this experiment, there is no evidence that Lewis acid sites convert to Brönsted acid sites upon introduction of a substantial amount of water (75 torr). Further experiments might reveal at what calcination temperature the surface becomes fully deprotonated so that only Lewis acid sites are present. The catalyst could then be investigated in terms of acid site conversion from Lewis to Brönsted acid sites. Improvements in the experimental technique such as more efficient charge compensation and use of pressed powder samples providing a smoother surface will enhance the quality of the data significantly in the future.

Two experiments were performed on other catalysts, i.e. γ-alumina and Nafion-H. These two samples were exposed to pyridine after being exposed to laboratory air. The samples were not evacuated at elevated temperature after pyridine adsorption, so more physisorbed pyridine is expected. Figure 65 shows the N 1s region for γ-alumina with adsorbed pyridine. The peak at a binding energy of 397.6 eV corresponds to pyridine coordinated to a Lewis acid site. No spectral peak is seen at higher binding energy, indicating that no Brönsted acid sites are present on this catalyst. This result agrees well with results of pyridine adsorption on γ-alumina obtained by IR-spectroscopy.

Figure 65. XPS of the N 1s region of the γ-alumina catalyst with adsorbed pyridine.

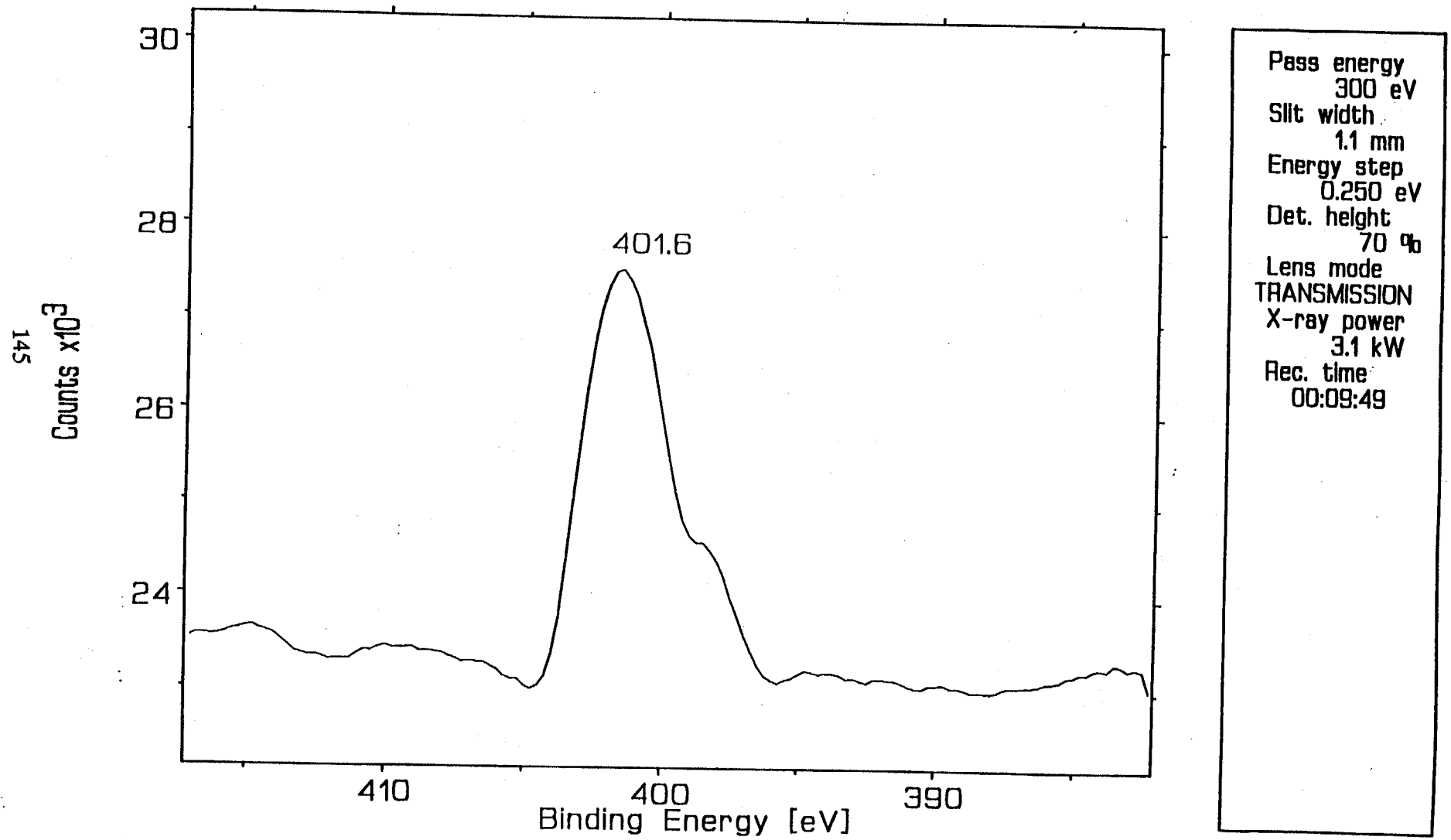

Figure 66 shows the N 1s binding energy region for Nafion-H with adsorbed pyridine. Nafion-H is a sulfonated polymer with a fluorocarbon backbone. Nafion-H is considered to be a Brönsted acid-containing material and is not expected to have any Lewis acid sites. In the XPS spectrum, the main peak is observed at 401.6 eV, which corresponds to a Brönsted acid site. A minor peak is evident in Figure 66 at 398.8 eV, and this is believed to be due to physisorbed pyridine. This peak would probably not be seen if the sample had been evacuated at elevated temperature prior to the analysis. The last two samples, γ-alumina and Nafion-H, indicate the validity of XPS as a method to distinguish and quantify Lewis and Brönsted acid sites.

F. Quantification of XPS Data: Amount of Sulfur on Sulfate-Modified Zirconia

The calculation of surface coverage has been performed such that it accounts for the mean free path of photoelectrons and instrumental constants. To determine the mean free path of the photoelectrons in the surface of the sample, the Chang equation (55) is used as given below.

Mean free path $(\lambda / = 0.2\ (E)^{0.5}\ t^0$

E = kinetic energy in eV

t^0 = monolayer thickness, which here is the spacing between the (100) layers of ZrO_2

The kinetic energy for Zr photoelectrons is 1304.4 eV and t^0 is 0.182 nm. Using these values yields a mean free path (escape depth) of 1.31 nm, which corresponds to about 7 layers. The mean free path and monolayer thickness values were used in the Dreiling equation (56), which gives a relationship between the measured photoelectron intensity and the atomic concentration on the surface. The equation considers attenuation effects due to surface overlayers of a certain thickness. The version of the Dreiling equation used for

Figure 66. XPS of the N 1s region of the Nafion-H catalyst with adsorbed pyridine.

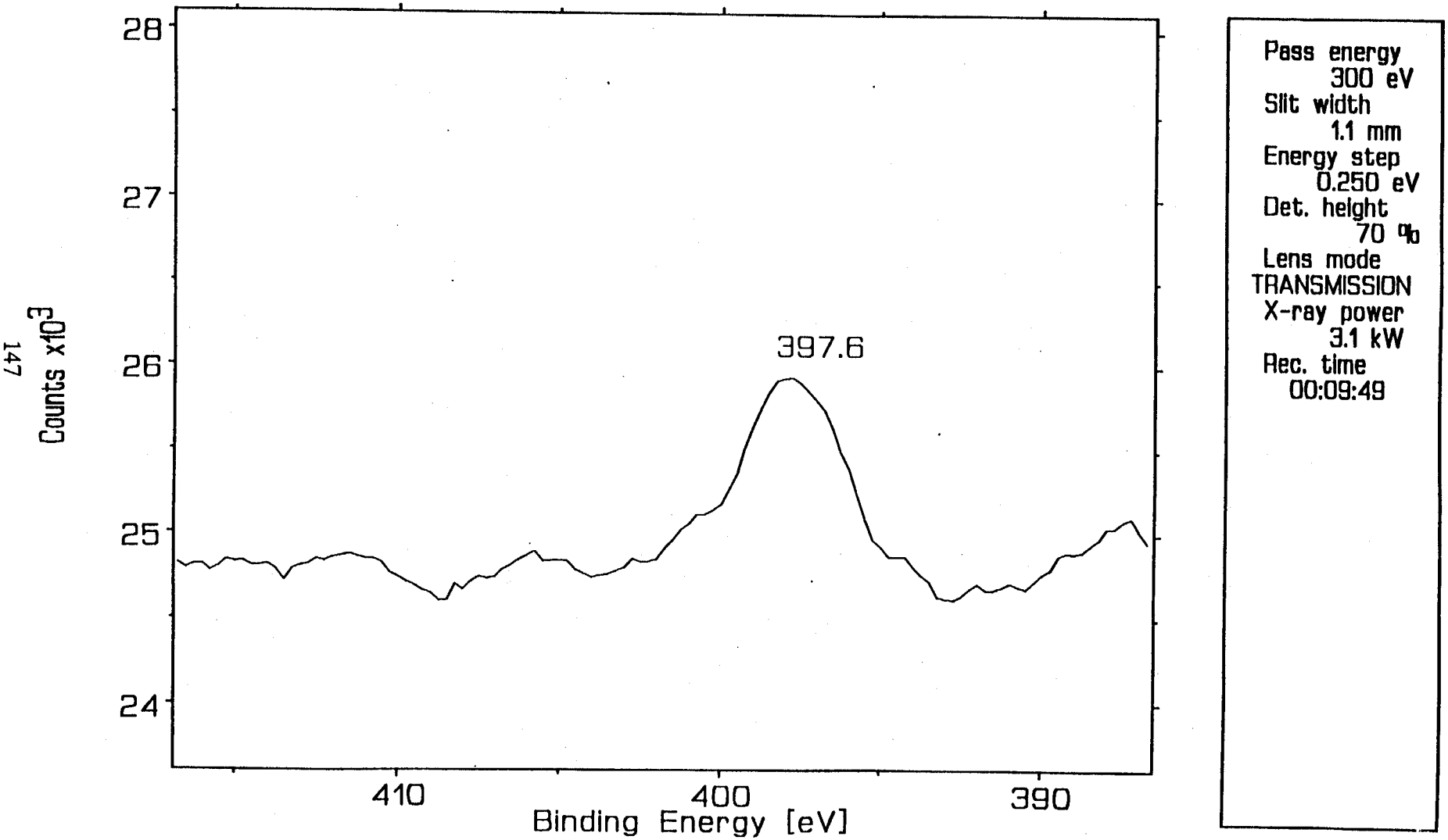

these calculations is the one utilized by Vedage et al. (57), as given below.

$$\frac{[S]}{[Zr]} = \frac{I_s}{I_{Zr}} \quad \frac{g\lambda_{Zr}}{t^0_{Zr}} \quad / \quad \left(\frac{\sigma_s}{\sigma_{Zr}} \frac{E_{Zr}}{E_S} + \frac{t^0_S}{t^0_{Zr}} \frac{I_S}{I_{Zr}} \right)$$

[S] = Concentration of sulfur on the surface
[Zr] = Concentration of zirconium on the surface
I = Measured photoelectron intensity
g = Escape angular factor for porous materials
λ = Mean free path
t^0_{Zr} = Monolayer thickness
t^0_S = Thermodynamic diameter of the sulfate anion (0.488 nm)
σ = Photoionization cross-section

The surface concentration ratio of [S]/[Zr] calculated with this method is 0.49. This value agrees very well with the value obtained with chemical elemental analysis, which resulted in a value of 0.55 assuming that all of the sulfur is on the surface of the sample. This provides confidence that the sulfate dopant is on the surface or associated with the outer-most surface layers and not with the bulk of the ZrO_2 catalyst.

Seah and Dench (58) have compiled values of measured mean free paths, as given in the literature, and have obtained an empirical equation for estimating the mean free path, $\lambda = B\,(E)^{1/2}$ for $E > 150$ eV and where B is a universal value for inorganic compounds (= 0.098). This gives a mean free path of 3.47 nm for zirconia. This general equation has an error of some 35%. Using this equation instead of the Chang equation for the mean free path yields a surface [S]/[Zr] ratio on the surface of 0.74, which is more sulfur than is available according to elemental analysis.

If a simple data treatment is used that does not account for screening processes due to the sulfate ion and to the angular factor, the surface [S]/[Zr] ratio will be higher than the available amount of sulfur. Therefore it appears that these considerations are important. The use of the Chang equation here is valid and will be used for all future experiments.

VII. Octane and Cetane Number Determination

A. Octane Number Determination

Octane number was determined for MIBE, MTBE, and a 50/50 by volume mixture of MIBE and MTBE. MIBE was produced by the Williamson ether synthesis. The preparation involves the formation of sodium butoxide from metallic sodium and isobutanol. Methyl iodide was added to form MIBE and sodium iodide. The product resulting from this synthesis was a 50/50 mixture of MIBE and isobutanol. For the purpose of octane number determination, this mixture was distilled under nitrogen to yield a >96% purity of MIBE, as determined by gas chromatography. The major impurity was isobutanol. MTBE was obtained from Aldrich Chem. Co. Determination of octane number was performed by Amoco Oil Company with ether samples found by us. The standard ASTM methods D-2699 and D-2700 were used for Research Octane Number and Motor Octane Number, respectively. The ether samples were tested for peroxides prior to octane determination. The peroxide level was <20 ppm for all three samples, which is considered to be acceptable. The ether samples were mixed with unleaded regular gasoline, where the amount of ether was 10% in the gasoline. The results obtained by Amoco Oil Co. are summarized in Table 21.

Table 21. Octane Numbers of MTBE and MIBE Gasoline Blends.

Sample	Research Octane Number	Motor Octane Number	Peroxide (ppm)
Unleaded Regular Gasoline (ULR)	92.1	82.3	-
10% MTBE in ULR	94.9	83.7	14
10% MTBE/MIBE in ULR	92.0	82.4	6
10% MIBE in ULR	88.8	80.8	17

MTBE increased the research octane number by 2.8 units and the motor octane number by 1.4 units, which is in good agreement with values obtained by Spindelbalker and Schmidt (59). MIBE, on the other hand, decreased the research octane number and motor octane number by 3.2 and 1.5 units, respectively. The gasoline/ether mixture containing the 1/1 by volume MIBE and MTBE had the same values as the base unleaded regular gasoline. In this case, an appreciable amount of oxygen was added to the ULR gasoline without altering its octane rating.

The blending octane numbers were calculated according to the following equation: Blending Research Number = RON (component A) × (percent component A) + RON (component B) × (percent component B). Table 22 lists the blending octane numbers for MIBE and MTBE. MTBE and MIBE are isomers, but it is clear from the results presented above that MTBE is superior to MIBE for octane enhancing purposes.

Table 22. Blending Research Octane Number (BRON) and Blending Motor Octane Number (BMON) of MTBE and MIBE in gasoline.

Sample	BRON	BMON
MTBE in ULR	120.1	96.3
MIBE in ULR	60.8	67.0

B. Cetane Number Determination

A 140 ml portion of MIBE was sent to Southwest Research Institute (SRI) for evaluation of the cetane number. The cetane number was reported to be 53. As commercial fuel in the U.S. is normally 40-45 cetane, MIBE shows promise as a high cetane additive should oxygenates be required in fuel as they are in gasoline fuels.

VIII. Experimental Methods

A. Calibration of Thermal Response Factors and GC Parameters

Thermal response factors (TRF) are necessary to quantitatively calculate amounts of products from the raw peak areas in gas chromatographic analysis when a thermal conductivity detector (TCD) is used. The raw peak area is divided by the thermal response factor to give the true response value.

Thermal response factors used in previous reports have not been determined in this laboratory, but literature values for reactants and products, as listed by Dietz (60), were utilized. However, it was found that the values from Dietz were not always satisfactory. New thermal response factors have been determined for methanol, isobutanol, methyl tert-butyl ether, dimethylether, and isobutene.

To avoid any interference from catalytic reactions, the reactor was filled with only 3 mm glass beads. Calibration was carried out at 123°C and ambient pressure. According to Dietz (60), thermal response factors are independent of temperature and flow rate. The flow of the internal standard, N_2, was carefully determined by several measurements using a bubble meter. Either dimethylether (DME) or isobutene was added and the total flow was measured. Liquid samples such as methanol (MeOH), isobutanol or methyl tert-butyl ether (MTBE) were introduced *via* a Gilson pump at a rate of 12.0 μl/min. Finally, helium, an inert carrier, was added to give a total flow of 5-6 l/hr.

Steady-state was reached within a 2 hr period and the calibration was allowed to run overnight to get a longtime average. Flows were very stable and the difference from injection to injection was kept to a minimum.

The new thermal response factors were determined in reference to the internal standard. This approach assumes that the thermal response factor for nitrogen is correct.

Nitrogen is a common internal standard in GC analysis, and therefore this assumption was accepted for this application. As can be seen from Table 23, the new thermal response factors were increased for isobutene and isobutanol by 13% and 19% respectively, while the thermal response factor for methanol decreased by 9%. The largest change was measured for dimethylether, which dropped 25%. The value for MTBE only changed by a difference of two units, which is within experimental error. Thermal response factors are not absolute values; rather they are instrumental values that will differ from system to system. It is also important to recognize that there is an age factor involved, meaning it is likely that the thermal response factors will change over time as the TCD ages. The new values for thermal response factors are used throughout this report.

Table 23. Thermal Response Factors of Pertinent Oxygenated Reagents and Products.

Compound	New TRF	Old TRF
Methanol	50	55
Isobutanol	115	97
MTBE	127	125
DME	75	100
Isobutene	93	82

GC Operating Conditions. The usual operating conditions that have been used to achieve separation of reaction products are given in Table 24. The column was a Wall Coated Open Tube (WCOT) capillary column with a chemically bonded 5.0 μm thick methyl silicone coating purchased from Chrompack Inc. These conditions allow for separation of

isobutene from both 1-butene and 2-butene. These three products are also separated from methanol and DME. Several iso-octenes can be separated from each other, but exact identification of the iso-octenes has yet to be resolved. C-8 ethers such as ditertiary butyl ether (DTBE) and diisobutyl ether (DIBE) can be resolved from one another, as well as from the iso-octenes. The chromatograms were not very well resolved towards the higher weight products, meaning after approx. 16 min, but two distinct groups of peaks could be seen. These groups are believed to be different kinds of C-12 compounds, and GC-MS will give a more complete identification of these products.

Table 24. Usual GC Operating Conditions

	Column pressure	0.5 MPa
	Injector temperature	250°C
	Detector temperature	275°C
Oven conditions:	Initial temperature	50°C
	Initial time	2 min
	Temp. ramp A	8°C/min to 110°C
	Hold time at 110°C	0 min
	Temp. ramp B	20°C/min to 250°C
	Hold time at 250°C	9 min
	Total analysis time	25 min

B. Gas Chromatographic Analysis with Mass Spectrometric Detection

Mass spectrometry is very useful in conjunction with gas chromatographic separation. It has the power of obtaining many spectra within a chromatographic peak, which can be used for detecting the products in unresolved GC peaks. It also serves as a more or less absolute indication of substances present in a mixture.

Reaction products from a standard test over Amberlyst-15 were collected in a cold trap and stored in a sealed container. The sample was transferred by syringe and analyzed by GC-MS using a similar column as mentioned above and the same operating conditions.